Available online at www.sciencedirect.com
SCIENCE DIRECT®
Journal of Solid State Chemistry 178 (2005) 1301–1307
JOURNAL OF SOLID STATE CHEMISTRY
www.elsevier.com/locate/jssc

Transport coefficients of titanium-doped Sb_2Te_3 single crystals

Č. Drašar[a,*], M. Steinhart[a], P. Lošťák[a], H.-K. Shin[b], J.S. Dyck[c,1], C. Uher[c]

[a]*Faculty of Chemical Technology, University of Pardubice, Čs. Legií Square 565, 532 10 Pardubice, Czech Republic*
[b]*Department of Physics, DMST, Ajou University, Korea*
[c]*Department of Physics, University of Michigan, Ann Arbor, MI 48109-1120, USA*

Received 24 November 2004; received in revised form 1 February 2005; accepted 7 February 2005

Abstract

Titanium-doped single crystals ($c_{Ti} = 0–2 \times 10^{20}$ atoms cm^{-3}) were prepared from the elements Sb, Ti, and Te of 5 N purity by a modified Bridgman method. The obtained crystals were characterized by measurements of the temperature dependence of the electrical resistivity, Hall coefficient, Seebeck coefficient and thermal conductivity in the temperature range of 3–300 K. It was observed that with an increasing Ti content in the samples the electrical resistivity, the Hall coefficient and the Seebeck coefficient increase. This means that the incorporation of Ti atoms into the Sb_2Te_3 crystal structure results in a decrease in the concentration of holes in the doped crystals. For the explanation of the observed effect a model of defects in the crystals is proposed. The data of the lattice thermal conductivity were fitted well assuming that phonons scatter on boundaries, point defects, charge carriers, and other phonons.

Keywords: Transport properties; $(Sb_{1-x}Ti_x)_2Te_3$; Point defects

1. Introduction

Antimony telluride Sb_2Te_3 is a layered semiconductor with tetradymite structure (space group D^5_{3d}). This compound is a component of materials that are used for the construction of thermogenerators and solid-state coolers [1]. Therefore, an investigation of the effect of various dopants on the physical properties of Sb_2Te_3 is interesting both for basic and applied research.

As grown single crystals of Sb_2Te_3 are invariably p-type semiconductors due to the existence of native defects characterized by the presence of Sb atoms on Te lattice sites, the so-called anti-site defects [2]. Only limited information is available on the influence of transition metal impurities on the properties of this material. It was found that manganese and iron impurities in Sb_2Te_3 crystals increase the concentration of holes [3–5]. According to the results of paper [6], Cr-doping in the Sb_2Te_3 crystals does not change the concentration of free current carriers, but their mobility decreases. Also the doping with vanadium does not change the concentration of holes in Sb_2Te_3. Nevertheless, a small content of vanadium in the Sb_2Te_3 crystals gives rise to their ferromagnetic behavior at low temperatures; the Curie temperature increases with vanadium content reaching approximately 22 K for $Sb_{1.97}V_{0.03}Te_3$ [7].

The analysis of reflectance spectra of Ti-doped Sb_2Te_3 crystals in the plasma resonance frequency region has shown that the presence of titanium decreases the concentration of holes in these crystals [8]. This conclusion was supported by measurements of the galvanomagnetic properties [9]. Nevertheless, the temperature dependence of the Seebeck coefficient, as well as the thermal conductivity, of Ti-doped Sb_2Te_3 crystals has not been studied.

In the present paper, samples of titanium-doped Sb_2Te_3 single crystals are characterized by

*Corresponding author. Fax: +420 466 036 033.
E-mail address: cestmir.drasar@upce.cz (C. Drašar).
[1]Present address: Department of Physics, John Caroll University, University Heights, OH 44118, USA.

0022-4596/$ - see front matter © 2005 Elsevier Inc. All rights reserved.
doi:10.1016/j.jssc.2005.02.005

measurements of the temperature dependence of electrical resistivity, Hall coefficient, Seebeck coefficient and thermal conductivity in the temperature range of 3–300 K. The aim is to find out how these transport properties are affected by incorporation of titanium atoms into the crystal lattice of Sb_2Te_3.

2. Experimental

The starting materials for growing the single crystals were prepared from the elements Sb, Te of 5 N purity, and $TiTe_2$. The synthesis of the polycrystalline $TiTe_2$ compound was carried out by heating a stoichiometric mixture of Ti and Te powders in an evacuated silica ampoule at 1400 K for 5 days. The X-ray diffractogram of the resulting product revealed only diffraction lines of the $TiTe_2$ compound. In the second step Ti-doped polycrystalline materials were prepared from the mixture of Sb, Te, and $TiTe_2$, corresponding to the atomic ratio (Sb + Ti):Te = 2:3, in silica ampoules evacuated to a pressure of 10^{-4} Pa. The synthesis was carried out in a horizontal furnace at 1073 K for 48 h. According to our experience with a range of transition metals (Ti, Zr, Hf, Cr, V…) the dissolution of a transition metal-telluride in liquid Sb_2Te_3 proceeds much faster than the reaction of Sb_2Te_3 with the transition metal. That is the reason why we use $TiTe_2$ instead of metallic Ti as a doping substance.

Finally, the single crystals were grown using the Bridgman method. A conical quartz ampoule, containing the synthesized polycrystalline material, was placed in the upper (warmer) part of the Bridgman furnace, where it was melted at 1003 K for 24 h. Then it was lowered into a temperature gradient of 400 K/5 cm at a rate of 1.3 mm/h. The single crystals were easily cleavable along the hexagonal planes (0001), i.e., perpendicular to the trigonal axis c which was parallel to the ampoule axis. Samples of dimensions $10 \times 3 \times 2\,mm^3$ (2 mm along the c-axis) were cut out from the middle part of the single crystals for physical property measurements. The concentration of titanium in these samples was determined by atomic emission spectrometry (AES). Seebeck coefficient (thermopower) and thermal conductivity were determined using a longitudinal steady-state technique in a cryostat equipped with a radiation shield. Thermal gradients were measured with the aid of fine chromel-constantan differential thermocouples, and a miniature strain gauge served as a heater. For the Seebeck probes we used fine copper wires that have previously been calibrated, and their thermopower contribution was subtracted from the measured sample thermopower. The Hall effect and electrical conductivity were studied using a Linear Research ac bridge with 16 Hz excitation in a magnet cryostat capable of fields up to 5 T. Measurements of these parameters were made over the temperature range of 3–300 K.

3. Results and discussion

3.1. Hall coefficient, electrical resistivity, Seebeck coefficient, and free carrier concentration

Temperature dependences of the Hall coefficient $R_H(B\|c)$, Seebeck coefficient $\alpha(\Delta T \perp c)$ and electrical resistivity $\rho_{\perp c}$ (all are in-plane measurements) are presented in Figs. 1–3. The values of these parameters at $T = 300$ K are summarized in Table 1. From the obtained results it can be seen that the incorporation of Ti atoms into the Sb_2Te_3 crystal structure results in an increase of all investigated parameters. The curves of $\alpha(\Delta T \perp c) = f(T)$ versus temperature of all the samples

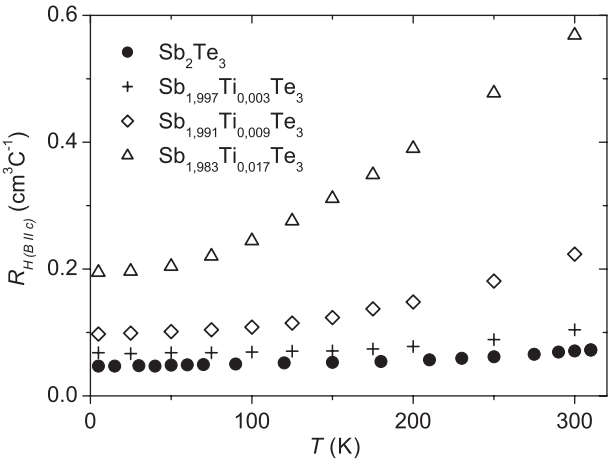

Fig. 1. Temperature dependence of the Hall coefficient $R_H(B\|c)$ of Ti-doped Sb_2Te_3 single crystals.

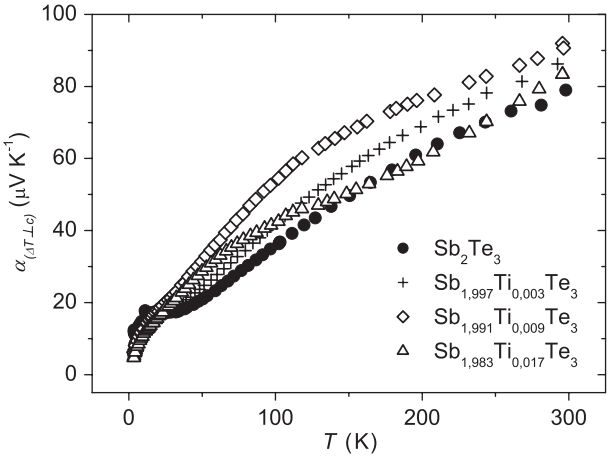

Fig. 2. Temperature dependence of the Seebeck coefficient $\alpha(\Delta T \perp c)$ of Ti-doped Sb_2Te_3 single crystals.

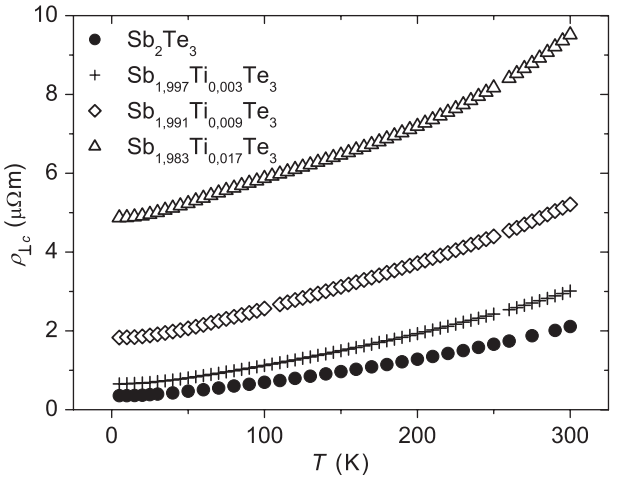

Fig. 3. Temperature dependence of the electrical resistivity $\rho_{\perp c}$ of Ti-doped Sb_2Te_3 single crystals.

Table 1
Values of the transport parameters at $T = 300\,K$ for $(Sb_{1-x}Ti_x)_2Te_3$ single crystals

No.	c_{Ti} ($10^{19}\,cm^{-3}$)	$\rho_{\perp c}$ ($\mu\Omega\,m$)	$R_H(B\|c)$ ($cm^3\,C^{-1}$)	$\alpha(\Delta T_{\perp c})$ (μVK^{-1})
1	0	2.12	0.07	79
2	1.90	3.05	0.11	88
3	5.75	5.21	0.22	91
4	10.74	9.53	0.57	84

are similar with an exception of the sample with the highest Ti content (see Fig. 2); we assume that the anomalous temperature dependence of this sample is associated with a change in the scattering mechanism of free carriers. The data imply that Ti-doping of Sb_2Te_3 crystals leads to a decrease in the concentration of holes. This result agrees well with the reflectance and galvanomagnetic measurements reported in papers [8,9]. The observed decrease in the hole concentration due to Ti doping can be explained by the substitution of Sb atoms with Ti atoms.

In order to evaluate the charges on the point defects we use the bonding model of Krebs [10]. According to this model, Sb and Te atoms in the Sb_2Te_3 crystals are linked together by σ-bonds with the participation of $5p$-orbitals of Sb and $5p$-orbitals of Te. The electron configuration of the valence sphere of Sb is $5s^25p^3$ and each Sb atom donates three electrons to the σ-bonds. Therefore, each Ti atom at the Sb lattice position should also donate three electrons to these bonds. As the electron configuration of Ti is $[Ar]3d^24s^2$ we assume that when a Ti atom occupies the Sb lattice position, its two $3d$ and two $4s$ electrons are excited into the nearby situated $4p$-orbitals; three of them take part in the formation of σ-bonds with Te atoms and the fourth electron is released into the conduction band. The substitutional defect, created in this way, is therefore singly positively charged and designated as $Ti^{\bullet}_{Sb}$. Such incorporation of the Ti-atoms into the Sb_2Te_3 crystal lattice can be described by the following scheme:

$$2Ti + 3Te \rightarrow 2Ti^{\bullet}_{Sb} + Sb_2Te_3 + 2e^{/}. \quad (1)$$

The recombination of the above electrons with holes results in the observed decrease in the concentration of free current carriers. This scheme is in accordance with the fact that all studied crystals are diamagnetic (Ti atoms are formally in the Ti^{4+} state).

The supposed incorporation of Ti atoms into the Sb-sublattice is supported by the results of X-ray diffraction [9] which confirm that an increasing content of Ti in Sb_2Te_3 leads to a decrease of the lattice parameters a and c and thus to a decrease of the unit cell volume. Noting that the crystal radius of Ti^{4+} ($r(Ti) = 0.0745\,nm$) is smaller than that of Sb^{3+} ($r(Sb) = 0.0900\,nm$) [11,12], the decrease in the unit cell volume is expected.

3.2. Thermal conductivity

The temperature dependence of the total thermal conductivity κ is given in Fig. 4. The values of κ for Sb_2Te_3 increase as temperature decreases and a peak develops at a temperature near 13 K. It is evident that the incorporation of Ti atoms into the Sb_2Te_3 crystal structure results in the suppression of the thermal conductivity at all temperatures.

Total thermal conductivity κ, in general, is the sum of two components; $\kappa = \kappa_L + \kappa_e$ where κ_e and κ_L are the electronic and lattice thermal conductivity contributions, respectively. The exact calculation of κ_e is complicated by the likely presence of two valence bands, the upper valence band (UVB) and the lower valence

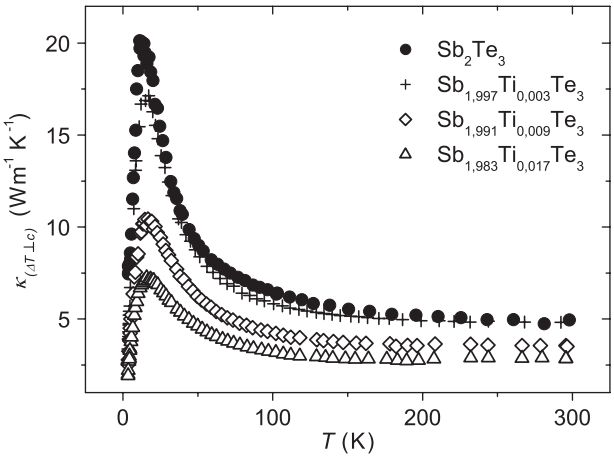

Fig. 4. Temperature dependence of the thermal conductivity $\kappa_{\perp c}$ of Ti-doped Sb_2Te_3 single crystals.

band (LVB) and hence of two kinds of holes. However, the two bands are not populated equally, the ratio of the LVB density of holes to that of the UVB hole density is equal to 390 [13]. In view of this large ratio, only the LVB holes are considered in further discussions.

The electronic component of the thermal conductivity κ_e was calculated from the experimental values of resistivity $\rho_{\perp c}$ using the Wiedemann–Franz relation $\kappa_e = LT/\rho_{\perp c}$, where L is the Lorenz number and T is the absolute temperature. In order to evaluate the effect of the scattering mechanism on the magnitude of κ_e, the value of the Lorenz number was determined from the general expression [1]:

$$L = \left(\frac{k_B}{e}\right)^2 \left\{ \frac{(s+7/2)F_{s+5/2}(\eta)}{(s+3/2)F_{s+1/2}(\eta)} - \left[\frac{(s+5/2)F_{s+3/2}(\eta)}{(s+3/2)F_{s+1/2}(\eta)}\right]^2 \right\}, \quad (2)$$

where a value of $s = -1/2$ corresponds to the scattering on acoustic phonons, $s = 1/2$ to the scattering on optical phonons and $s = 3/2$ to the scattering on ionized impurities. The required values of the reduced Fermi level η were calculated from the experimental values of the Seebeck coefficient using the expression [14]:

$$\alpha = \pm\frac{k_B}{e}\left(\frac{(s+5/2)F_{s+3/2}(\eta)}{(s+3/2)F_{s+1/2}(\eta)} - \eta\right). \quad (3)$$

Since the temperature dependence of the Seebeck coefficient at temperatures below 50 K is influenced by phonon drag, the calculations were carried out only for temperatures above 50 K. One can compare the influence of several scattering mechanisms on the electronic thermal conductivity of Sb_2Te_3 in Fig. 5. We see hardly any difference between the result calculated with the constant value of the Lorenz number $L = L_0 = \pi^2/3(k_B/e)^2$ (degenerate system), and the results obtained assuming non-degenerate systems with a variety of scattering mechanisms acting below 100 K. So in the first approximation we use the Wiedemann–Franz relation $\kappa_e = L_0 T/\rho$ to calculate κ_e in this temperature region. Subtracting the electronic thermal conductivity contribution from the total measured thermal conductivity we obtain the lattice thermal conductivity displayed in Fig. 7.

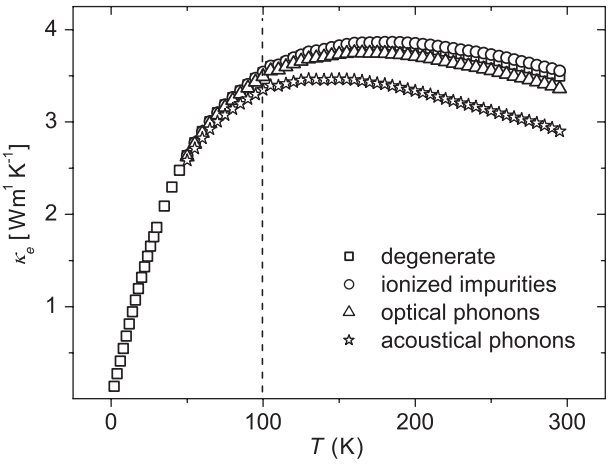

Fig. 5. Temperature dependence of the electronic part of thermal conductivity κ_e of Sb_2Te_3 single crystals assuming various scattering mechanisms.

Temperature dependence of lattice thermal conductivity can be fitted within Debye approximation using the following expression [14]:

$$\kappa_L(T) = \frac{k_B}{2\pi^2 v}\left(\frac{k_B T}{\hbar}\right)^3 \int_0^{\theta_D/T} \tau_C \frac{y^4 e^y}{(e^y-1)^2}\,dy, \quad (4)$$

where k_B is the Boltzmann constant, $\hbar$ is the reduced Planck constant, y stands for the dimensionless parameter $y = \hbar\omega/k_B T$, ω is the phonon frequency, θ_D is Debye temperature, v is the velocity of sound, and τ_C is the phonon relaxation time. This relaxation time can be written in terms of the individual scattering times accounting for various scattering processes as follows:

$$\tau_C^{-1} = \frac{v}{d} + A\omega^4 + B\omega^2 T \exp\left(-\frac{\theta_D}{3T}\right) + C\omega. \quad (5)$$

Here d is the crystal dimension ($d = 2$ mm for the smallest dimension of our crystals) and the coefficients A, B, and C are temperature independent fitting parameters. The terms in Eq. (5) stand for boundary, point-defect, three-phonon umklapp, and carrier-phonon scattering, respectively. The first three terms account for phonon scattering in dielectric crystals. The fourth term represents relaxation time for scattering of phonons by free carriers in a parabolic band as derived by Ziman [15]. This term holds provided that $l_h \gg \lambda_{ph}$ where l_h is the mean free path of free carriers (holes) and λ_{ph} is the phonon wavelength. In Fig. 6, we show the comparison of l_h and λ_{ph} estimated using the formal Drude analysis of the transport data and the dominant phonon method, respectively, for Ti-doped Sb_2Te_3. This illustrates that Eq. (5) is appropriate for Sb_2Te_3 while the doped samples may not fully satisfy the assumption in which case the underlying theory might possibly break down [16]. Going from $l_h \gg \lambda_{ph}$ to $\lambda_{ph} \gg l_h$, τ_C becomes proportional to ω^2 rather than ω and consequently temperature dependence of κ_L becomes proportional to T rather then to T^2 in the respective temperature region (see Fig. 6). In spite of the fact that the phonon mean free path of the doped samples might not satisfy the condition $l_h \gg \lambda_{ph}$, leaving the last term out yields poor fits.

To make use of Eq. (4), one needs the Debye temperature θ_D. In fact, this temperature is strictly not a constant but is temperature dependent. While $\theta_D(T)$ is known for Bi_2Te_3 [17,18], the corresponding

temperature dependence for Sb_2Te_3 is not available. We make here an assumption that, while different in magnitude, the $\theta_D(T)$ of both Bi_2Te_3 and Sb_2Te_3 are similar in their temperature dependence. Correspondingly, the temperature dependence of θ_D (Bi_2Te_3) was shifted to fit the value of θ_D (Sb_2Te_3) at 160 K and this dependence was fitted. The obtained polynomials

$$\theta_D(T = 2 - 8\,\mathrm{K}) = 107.617 + 1.291T - 0.008T^2,$$
$$\theta_D(T = 8 - 100\,\mathrm{K}) = 91.258 + 3.188 - 0.064T^2 + 5.895e - 4T3 - 2.008e - 6T^4.$$

were used for fitting of κ_L.

The sound velocity was estimated from [19] to be $v = 2900\,\mathrm{ms}^{-1}$. The results of the fit are summarized in Table 2 and in Fig. 7. Upon inspecting fitting parameters in Table 2, it is evident that the point defect scattering parameter A controls the behavior. It can be written as [20]

$$A = \frac{\Omega\Gamma}{4\pi v^3}, \tag{6}$$

where Ω is the unit cell volume (for Sb_2Te_3 $\Omega = 0.161\,\mathrm{nm}^3$), Γ is the scattering parameter which for a compound A_aB_b can be written as [21]

$$\Gamma(A_aB_b) = \frac{a}{a+b}\left(\frac{M_A}{M_m}\right)^2\Gamma(A) + \frac{b}{a+b}\left(\frac{M_B}{M_m}\right)^2\Gamma(B), \tag{7}$$

where M_m is the mean atomic mass of atoms composing the compound, $M_m = (aM_A + bM_B)/(a+b)$. $\Gamma(A,B)$ is the scattering parameter of the substitutional impurity at a respective site:

$$\Gamma(A,B) = \alpha(1-\alpha)[(\Delta M/M_{ave})^2 + \varepsilon(\Delta\delta/\delta_{ave})^2]. \tag{8}$$

Here α ($\alpha = x$ in this case) is the relative concentration of impurity at a respective site, $\Delta M = M_i - M(A,B)$ is the atomic mass difference between the impurity and the atom normally associated with that lattice site, $\Delta\delta = \delta_I - \delta$ is the difference in radii between the impurity and the atom normally associated with that lattice site, M_{ave} and δ_{ave} are the weighted averages of mass and radius at that lattice site, respectively, and ε is a phenomenological parameter. The first term of Eq. (8) accounts for mass fluctuation and the second term accounts for atomic radius fluctuations, i.e., elastic strain.

The exact radii of Sb and Ti in Sb_2Te_3 are unknown. The average distance between Sb and Te in the compound (0.311 nm) would rather support an ionic crystal picture ($r(Sb^{+3}) + r(Te^{-2}) = 0.090 + 0.207$ nm), as opposed to a covalent one ($r(Sb) + r(Te) =$

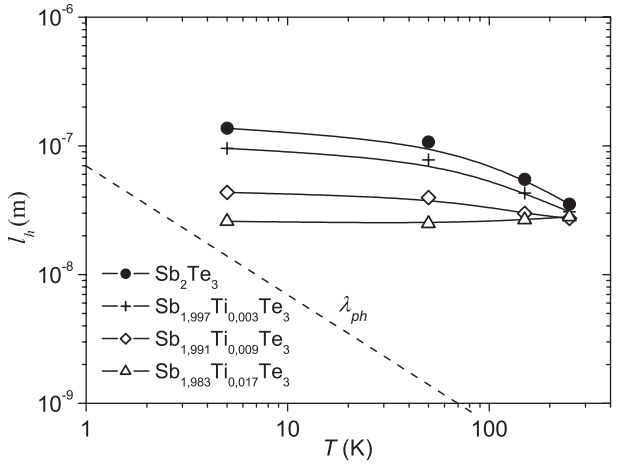

Fig. 6. Estimated hole mean free path l_h and phonon wavelength λ_{ph} as a function of temperature for Ti-doped Sb_2Te_3 single crystals.

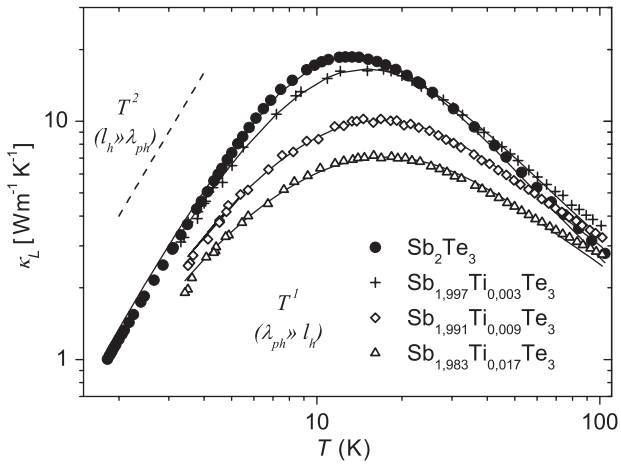

Fig. 7. Lattice thermal conductivity for Ti-doped Sb_2Te_3 single crystals. Solid lines are theoretical fits to Eqs. (4) and (5).

Table 2
Fitting parameters for theoretical analysis of lattice thermal conductivity of $(Sb_{1-x}Ti_x)_2Te_3$ single crystals as they refer to Eqs. (4) and (5)

No.	x (actual)	A (10^{-43} s^3)	B (10^{-18} s K^{-1})	C (10^{-4})
1	0	9.65	27	0.82
2	0.0015	17.6	20	0.85
3	0.0046	55.5	17	1.03
4	0.0086	113	16	1.11

Table 3
Values of the parameter ε and the ratio R of $(Sb_{1-x}Ti_x)_2Te_3$ single crystals resulting from the analysis of parameter , see text for details

No.	x (actual)	ε	R
2	0.0015	183	14.7
3	0.0046	192	15.4
4	0.0086	211	16.9

0.137 + 0.136 nm). Therefore we use ionic crystal values for all elements, including $r\,(Ti^{+4}) = 0.0745$ nm [11,12].

The ε parameter and the ratio of strain field to mass fluctuation effects $R = \varepsilon(\Delta\delta/\delta_{ave})^2/(\Delta M/M_{ave})^2$ are summarized in Table 3. The experimentally determined Ti content (AES-value) was used in the evaluation. The R-values indicate that strain field plays a more important role than mass fluctuations.

The parameter B of the umklapp scattering term in Eq. (5) is written as [22]

$$B = \frac{n^{2/3}\hbar\gamma^2}{M\theta_D v^2}. \tag{9}$$

This is a semi-empirical formula where γ is the Grüneisen parameter, M is the average atomic weight, and n is the number of atoms in a molecule, here $n = 5$. We observe a small decrease of B with increasing Ti concentration, see Table 2. A possible explanation is that titanium stiffens the lattice and increases the value of both θ_D and v. We note that the measurement of microhardness shows a roughly 20% increase for the highest Ti concentration.

The parameter C of carrier-phonon scattering can be written as [23]

$$C = \frac{(\xi m^*)}{2\pi\hbar^3\rho v}, \tag{10}$$

where ξ is the deformation potential, m^* is the hole effective mass and ρ the density. We observe a small enhancement in the parameter C with increasing Ti concentration. A possible explanation of the enhancement is the increase in the effective mass due to the decreasing hole concentration. The upper valence band (light holes) is filling up and becomes even less evident in transport properties of the Ti-doped samples in comparison to pure Sb_2Te_3. This means that the hole effective mass increases due to a stronger influence of the lower valence band (heavy holes). Similar conclusions were made for other Sb_2Te_3-doped crystals based on Shubnikov–de Haas effect measurements presented in [9,13]. It is to be noted however that though we see a clear trend regarding the value of parameter C, the enhancement is of the same order of magnitude as the estimated error.

4. Conclusions

From the results of the measurements of transport coefficients of Ti-doped Sb_2Te_3 crystals we have come to the following conclusions:

1. Doping of Sb_2Te_3 crystals by Ti-atoms results in a marked decrease in the hole concentration. This means that Ti can be used as an effective dopant for thermoelectric applications. We assume that this effect is due to the incorporation of Ti atoms into the Sb-sublattice and the formation of positively charged substitutional defects $Ti^{\bullet}_{Sb}$.
2. Lattice thermal conductivity was fitted well assuming that phonons scatter on boundaries, point defects, charge carriers, and other phonons within the Debye approximation. Incorporation of Ti-atoms into Sb_2Te_3 crystal lattice affects primarily point defect scattering.

Acknowledgments

The research was supported by Ministry of Education of Czech Republic under the project KONTAKT ME 513 and by the NSF Grant INT 0201114.

References

[1] G.S. Nolas, J. Sharp, H.J. Goldsmid, Thermoelectrics, Basic Principles and New Materials Developments, Springer, Berlin, Heidelberg, 2001, p. 111.
[2] H. Scherrer, S. Scherrer, Thermoelectric Materials, CRC Press, Inc., Boca Raton, FL, 1995, pp. 211–237.
[3] J. Horák, M. Matyáš, L. Tichý, Phys. Status Solidi (a) 27 (1975) 621.
[4] J.S. Dyck, P. Švanda, P. Lošťák, J. Horák, W. Chen, C. Uher, J. Appl. Phys. 94 (2003) 7631.
[5] P. Švanda, P. Lošťák, Č. Drašar, J. Navrátil, L. Beneš, T. Černohorský, Radiat. Eff. Def. Solids 153 (2000) 59.
[6] P. Lošťák, Č. Drašar, J. Navrátil, L. Beneš, Cryst. Res. Technol. 31 (1996) 403.
[7] J.S. Dyck, P. Hájek, P. Lošťák, C. Uher, Phys. Rev. B 65 (2002) 115212.
[8] Č. Drašar, P. Lošťák, J. Navrátil, T. Černohorský, V. Mach, Phys. Stat. Sol. (b) 191 (1995) 523.
[9] V.A. Kulbachinskii, N. Miura, H. Nakagawa, Č. Drašar, P. Lošťák, J. Phys.: Condens. Matter 11 (1999) 5273.
[10] H. Krebs, Grundzüge der anorganischen Kristallchemie, F. Enke, Stuttgart, 1968, p. 239.
[11] R.D. Shannon, Acta Crystallogr. A 32 (1976) 751.
[12] L. Pauling, The Nature of the Chemical Bond, Cornell University Press, 1961.
[13] V.A. Kulbachinskii, Z.M. Dashevskii, M. Inoue, M. Sasaki, H. Negishi, W.X. Gao, P. Lošťák, J. Horák, A. de Visser, Phys. Rev. B 52 (1995) 10915.
[14] J. Callaway, Phys. Rev. 113 (1959) 1046.
[15] J.M. Ziman, Electrons and Phonons, Clarendon, Oxford, UK, 1960.
[16] A.B. Pippard, Philos. Mag. 46 (1955) 1104.

[17] P.V. Gultyaev, A.V. Petrov, Sov. Phys. Solid State 1 (1959) 330.
[18] G.E. Shoemake, J.A. Rayne, R.W. Ure, Phys. Rev. 185 (1969) 1046.
[19] J.S. Dyck, W. Chen, C. Uher, C. Drasar, P. Lostak, Phys. Rev. B 66 (2002) 125206.
[20] P.G. Klemens, Proc. Phys. Soc. London A 68 (1955) 1113.
[21] B. Abeles, Phys. Rev. 131 (1963) 1906.
[22] G.A. Glassenbrenner, G.A. Slack, Phys. Rev. 134 (1964) 1058.
[23] J.E. Parrott, A.D. Stuckes, Thermal Conductivity of Solids, Pion Limited, London, 1975, p. 68.